Available online at www.sciencedirect.com

ScienceDirect

Current Opinion in Neurobiology

From the statistics of connectivity to the statistics of spike times in neuronal networks

Gabriel Koch Ocker[1,a], Yu Hu[2,a], Michael A Buice[1,3], Brent Doiron[4,5], Krešimir Josić[6,7,8], Robert Rosenbaum[9] and Eric Shea-Brown[1,3,10]

An essential step toward understanding neural circuits is linking their structure and their dynamics. In general, this relationship can be almost arbitrarily complex. Recent theoretical work has, however, begun to identify some broad principles underlying collective spiking activity in neural circuits. The first is that local features of network connectivity can be surprisingly effective in predicting global statistics of activity across a network. The second is that, for the important case of large networks with excitatory-inhibitory balance, correlated spiking persists or vanishes depending on the *spatial scales* of recurrent and feedforward connectivity. We close by showing how these ideas, together with plasticity rules, can help to close the loop between network structure and activity statistics.

Addresses
[1] Allen Institute for Brain Science, United States
[2] Center for Brain Science, Harvard University, United States
[3] Department of Applied Mathematics, University of Washington, United States
[4] Department of Mathematics, University of Pittsburgh, United States
[5] Center for the Neural Basis of Cognition, Pittsburgh, United States
[6] Department of Mathematics, University of Houston, United States
[7] Department of Biology and Biochemistry, University of Houston, United States
[8] Department of BioSciences, Rice University, United States
[9] Department of Mathematics, University of Notre Dame, United States
[10] Department of Physiology and Biophysics, and University of Washington Institute for Neuroengineering, United States

Corresponding author: Shea-Brown, Eric (etsb@amath.washington.edu)
[a] Equal contribution.

Current Opinion in Neurobiology 2017, **46**:109–119

This review comes from a themed issue on **Computational neuroscience**

Edited by **Adrienne Fairhall** and **Christian Machens**

For a complete overview see the Issue and the Editorial

Available online 30th August 2017

http://dx.doi.org/10.1016/j.conb.2017.07.011

Introduction

Here, we focus on relating network connectivity to collective activity at the level of spike times, or *correlations* in neurons' spike trains (see Box 1). Such correlations are known to have complex but potentially strong relations with coding in single neurons [1] and neural populations [2–5], and can modulate the drive to a downstream population [6]. Moreover, such correlated activity can modulate the evolution of synaptic strengths through spike timing dependent plasticity (STDP) ([7,8••,9], but see [10]).

Collective spiking arises from two mechanisms: connections among neurons within a population, and external inputs or modulations affecting the entire population [11–13]. Experiments suggest that both are important. Patterns of correlations in cortical micro-circuits have been related to connection probabilities and strengths [14]. At the same time, latent variable models of dynamics applied to cortical data have revealed a strong impact of global inputs to the population [15,16••,17,18].

At first, the path to understanding these mechanisms seems extremely complicated. Electron microscopy (EM) and allied reconstruction methods promise connectomes among thousands of nearby cells, tabulating an enormous amount of data [19–25]. This begs the question of what *statistics* of connectivity matter most — and least — in driving the important activity patterns of neural populations. The answer would give us a set of meaningful 'features' of a connectome that link to basic statistical features of the dynamics that such a network produces. Our aim here is to highlight recent theoretical advances toward this goal.

Mechanisms and definitions: sources and descriptions of (co)variability in spike trains

Neurons often appear to admit spikes stochastically. Such variability can be due to noise from, for example, synaptic release [28], and can be internally generated via a chaotic 'balanced' state [29,30,31••]. As a consequence, the structure of spike trains is best described statistically. The most commonly used statistics are the instantaneous firing rate of each neuron, the autocorrelation function of the spike train (the probability of observing pairs of spikes in a given cell separated by a time lag s), and the cross-correlation function (likewise, for spikes generated by two different cells). As shown in Box 1, even weak correlations yield coherent, population-wide fluctuations in spiking activity that can have a significant impact on

Box 1 Spike train statistics.

The spike train of neuron i is defined as a sum of delta functions, $y_i(t) = \sum_k \delta(t - t_i^k)$; t_i^k is the time of neuron i's kth spike. Spike train moments can be obtained from samples of the spike trains of each neuron in a population. The first spike train moment is the instantaneous firing rate, $\langle y_i(t) \rangle$. The angular brackets $\langle\rangle$ denote an average over trials. The correlation of two spike trains is $\mathbf{m}_{ij}(t_i, t_j) = \langle y_i(t_i) y_j(t_j) \rangle$. If $i = j$ it is an autocorrelation, otherwise a cross-correlation. In general a nth order correlation, or moment, of n spike trains, is defined as a trial-average of products of those spike trains:

$$\mathbf{m}_{i,j,\ldots,n}(t_i, \ldots, t_n) = \langle \prod_{i=1}^{n} y_i(t_i) \rangle \tag{1}$$

In practice, time is discretized into increments of size Δt, and spike trains are binned. Equation 1 is recovered from its discrete counterpart in the limit $\Delta t \to 0$. If the spike trains are stationary (their statistics do not change over time) we can replace averages over trials with averages over time. The correlation in this case only depends on the *time lag* in between spikes:

$$\mathbf{m}_{i,j,\ldots,n}(s_j, \ldots, s_n) = \frac{1}{T} \int_0^T dt_i \, y_i(t_i) \prod_{j=i+1}^{n} y_j(t_i + s_j) \tag{2}$$

where $s_j = t_j - t_i$ for $j = i + 1, \ldots, n$. The correlation function measures the frequency of spike pairs. Two uncorrelated Poisson processes with rates r_i and r_j have $\mathbf{m}_{ij}(s) = r_i r_j$, independent of the time lag s. The statistics of any linear functional of the spike trains (such as output spike counts, or synaptic outputs or inputs) can be derived from these spike train statistics [16••,26••].

The joint moments of the spike trains in a population also determine the variability and temporal correlations of the population-averaged activity, $y(t) = \frac{1}{N} \sum_{i=1}^{N} y_i(t)$. The average over the population can be interchanged with the average over trials and product over neurons in Equation 1 so that a mth order moment of the population activity, y, is given by:

$$m(t_i, \ldots, t_m) = \frac{1}{N^m} \sum_{1 \le j_1, \ldots, j_m \le N} \mathbf{m}_{j_1, \ldots, j_m}(t_i, \ldots, t_m)$$

Even weak correlations in $\mathbf{m}$ can give rise to strong population fluctuations (**Panel A**).

Finally, moments mix interactions of different orders. To account for lower-order contributions, we can define *cumulants* of the spike trains. The first cumulant and the first moment both equal the instantaneous firing rate. The second cumulant is the covariance function of the spike train: $\mathbf{C}_{ij}(s) = \mathbf{m}_{ij}(s) - r_i r_j$. The third spike train cumulant similarly measures the frequency of triplets of spikes, above what could be expected by composing those triplets of individual spikes and pairwise covariances. Higher order cumulants have similar interpretations [27].

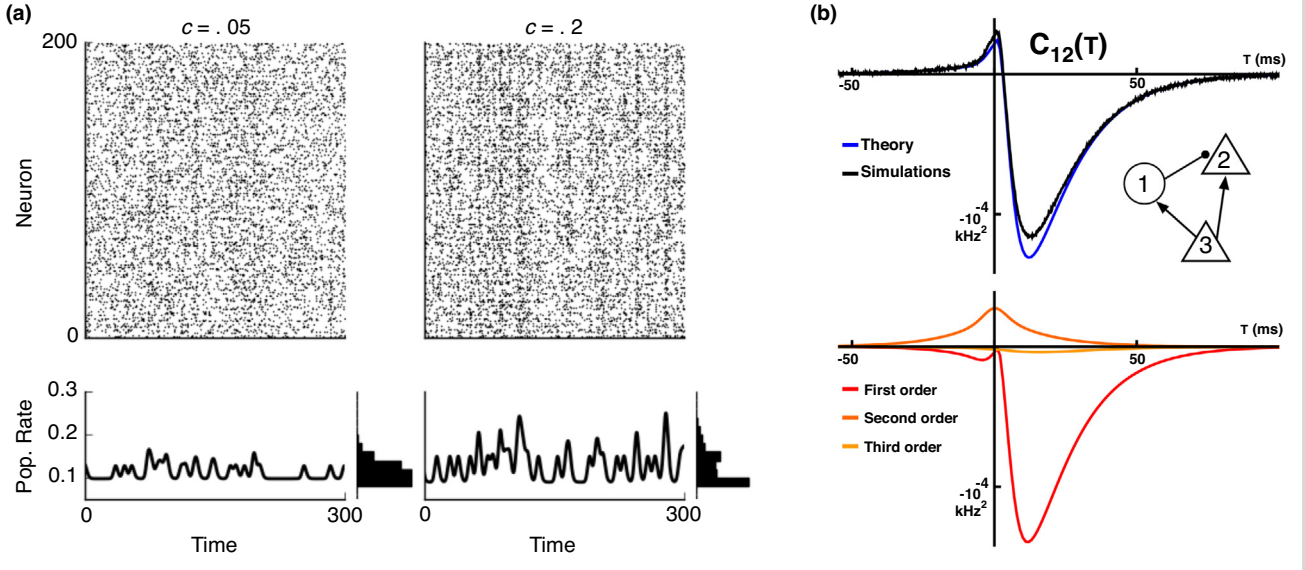

Pairwise correlations and population variability. (a) Variability of the population-averaged activity in 200 uncoupled integrate-and-fire neurons receiving white noise inputs with different strengths of spatial input correlation. (b) Cross-covariance of two neurons' spike trains in a feed-forward microcircuit with two excitatory (cell 2,3) and one inhibitory (cell 1) neurons. Top: simulation of (black) versus linear response theory (blue; Equation 6). Bottom: contribution of different length paths through the microcircuit (Equation 8). Adapted from [38•].

cells downstream [6]. Similarly, higher-order correlations are related to the probability of observing triplets, quadruplets or more spikes in a group of neurons, separated by a given collection of time lags (Box 1).

Spike train covariability from recurrent connectivity and external input

In recent years, neuroscientists have advanced a very general framework for predicting how spike train

correlations (more specifically, cumulants; Box 1) depend on the structure of recurrent connectivity and external input. This framework is based on *linearizing the response* of a neuron around a baseline state of irregular firing. For simplicity, we will present this in the temporal Fourier domain; the time-domain equations have similar forms with integrals over time. Assuming that each neuron linearly filters its synaptic inputs, and that in the absence of correlating inputs from the model network or external sources it has a baseline spike train $y_i^0(\omega)$, we can write its spike train $y_i(\omega)$ as:

$$y_i(\omega) = \underbrace{y_i^0(\omega)}_{\text{baseline}} + A_i(\omega)\Big(\underbrace{\xi_i(\omega)}_{\text{external}} + \underbrace{\sum_j \mathrm{W}_{ij}(\omega) y_j(\omega)}_{\text{internal}}\Big) \tag{3}$$

Here, $A_i(\omega)$ is the linear response of neuron i's *trial-averaged* rate to a perturbation in its synaptic input (Fourier transform of its impulse response, or PSTH [34]), and $\xi_i(\omega)$ is an external signal to neuron i. Finally, the network is described by its synaptic weight matrix $\mathbf{W}(\omega)$; $\mathrm{W}_{ij}(\omega)$ encodes the weight and time-course of synaptic connections from neuron j to neuron i. Below, we will suppress the ω-dependence of all variables for ease of notation.

We will use the linear response ansatz of Equation 3 to calculate trial-averaged spike train statistics. The simplest such is the firing rate. Collecting the spike trains y_i in the vector $\mathbf{y}$ (and similar for $\mathbf{y}^0$ and $\boldsymbol{\xi}$), we can average over trials in Equation 3 to obtain:

$$\langle \mathbf{y} \rangle = (\mathbf{I} - \mathbf{K})^{-1}\big(\langle \mathbf{y}^0 \rangle + \mathbf{A}\langle \boldsymbol{\xi} \rangle\big) \tag{4}$$

where $\langle\ \rangle$ denotes an average over trials. We have defined the effective interaction matrix $\mathbf{K}_{ij} = \mathbf{A}_{ii}\mathbf{W}_{ij}$ of synaptic weights weighted by the postsynaptic response gain. The first factor on the right-hand side of Equation 4 is

$$\boldsymbol{\Delta} \equiv (\mathbf{I} - \mathbf{K})^{-1}. \tag{5}$$

Δ_{ij} determines how the baseline and externally-driven activity of neuron j propagates through the network to impact neuron i's activity. We call Δ_{ij} a *propagator*.

Finally, we can also use Equation 3 to calculate the correlations between neurons' activities. For simplicity, we remain in the temporal Fourier domain and present the result as a matrix of spike train *auto-* and *cross-spectra*, $\mathbf{C}(\omega)$; this is the matrix of the Fourier transforms of the familiar auto- and cross-covariance functions. The auto- (cross-) spectra correspond to diagonal (off-diagonal) terms of $\mathbf{C}(\omega)$. In particular, evaluated at $\omega = 0$, these terms give the variance and co-variance of spike counts over any time window large enough to contain the underlying auto and cross-correlation functions [32,33]. The spectral matrix $\mathbf{C}(\omega)$ is given by:

$$\mathbf{C} = \underbrace{\boldsymbol{\Delta}\mathbf{C}^0\boldsymbol{\Delta}^*}_{\text{internal}} + \underbrace{\boldsymbol{\Delta}(\mathbf{A}\mathbf{C}^{\text{ext}}\mathbf{A}^*)\boldsymbol{\Delta}^*}_{\text{external}} \tag{6}$$

where * denotes the conjugate transpose. The matrix $\mathbf{C}^0$ is diagonal, containing the power spectrum of each neuron's baseline spike train y_i^0. The first term thus describes how the baseline variable spike emission propagates through the network to give rise to correlated activity in pairs of neurons.

The second right-hand side term of Equation 6 describes how correlated external inputs give rise to correlated activity. The correlation of the external inputs to different neurons, ξ_i and ξ_j, is described by their cross-spectrum $\mathbf{C}_{ij}^{\text{ext}}$. The direct impact of external inputs on joint activity in their targets is $(\mathbf{A}\mathbf{C}^{\text{ext}}\mathbf{A}^*)$. The multiplication with $\boldsymbol{\Delta}$ and $\boldsymbol{\Delta}^*$ then describes how that externally-driven joint activity propagates through the network.

In the simplest case of an uncoupled pair of neurons i and j receiving common inputs, Equation 6 reduces to $\mathbf{C}_{ij}(\omega) = \mathbf{A}_i(\omega)\mathbf{C}_{ij}^{\text{ext}}(\omega)\mathbf{A}_j(-\omega)$ [32,36]. The covariance of the two spike trains is thus given by the input covariance, multiplied by the gain with which each neuron transfers those common inputs to its output. Analyses of uncoupled neurons have also yielded insight into the mechanisms for higher-order spike train correlations and the distribution of population activity [89,90].

Equation 6 has a rich history: Sejnowski used a similar expression in describing collective fluctuations in firing rate networks [40]. Linder, Doiron, Longtin and colleagues derived this expression in the case of stochastically driven integrate and fire neurons [41,42], an approach generalized by Trousdale *et al.* [38•] (see a comparison between the linear response approximation Equation 7 and simulation of exponential integration-and-fire neurons in Box 1, Panel B). Hawkes derived an equivalent expression for the case of linearly interacting point processes (now called a multivariate Hawkes process), as pointed out by Pernice *et al.*, who applied and directly related them to neural models [37••,43,44]. The correspondence of the rate dynamics of the Hawkes model, networks of integrate-and-fire neurons, and binary neuron models, was discussed in detail in [45] and the direct approximation of integrate-and-fire neurons by linear-nonlinear-Poisson models in [46].

Moreover, Buice and colleagues [47] developed a field theoretical method that encompasses the above approach and extends the formulation to correlations of arbitrary order. Importantly, this also allows for nonlinear interactions. An expansion can be derived via this method that

describes the coupling of higher order correlations to lower moments: in particular, pairwise correlations can impact the activity predicted from mean field theory [26••]. The field theoretic approach has also been applied to models of coupled oscillators related to neural networks, specifically the Kuramoto model [48,49] and networks of 'theta' neurons [50]. Similarly, Rangan developed a motif expansion of the operator governing the stationary dynamics of an integrate-and-fire network [51•].

We have presented the linear response theory for spike train covariances in the context of linearizing neurons' activity around a baseline stationary state. This theory thus requires access to knowledge of the fluctuations of the baseline state, $\mathbf{C}^0$, and linear response functions $\mathbf{A}$. In large networks, internally generated variability can be temporally correlated which presents a complication [85,86]. When connections are sufficiently strong, this slow variability can reflect a loss of stability of the baseline state [88,91,92]. The predictions of the baseline single-neuron spiking activity and linear response in the face of slow internally-generated fluctuations pose additional challenges which have just begun to be explored [87].

Finally, a global modulation in the activity of many neurons due to shifts in attention, vigilance state, and/or motor activity, would result in low-rank matrix $\mathbf{C}^{\text{ext}}$. In this case the second, external term of Equation 6 will itself be low rank, since the rank of a matrix product $\mathbf{AB}$ is bounded above by the ranks of $\mathbf{A}$ and $\mathbf{B}$. Experimentally obtained spike covariance matrices can be decomposed into a low-rank and 'residual' terms [35,15] that could correspond to the two terms in the matrix decomposition Equation 6.

Network motifs shape collective spiking across populations

In order to investigate the synaptic interactions contributing to the propagator matrix $\mathbf{\Delta}$, we can expand it in powers of the interaction matrix $\mathbf{K}$ as

$$\mathbf{\Delta} = \sum_{m=0}^{\infty} \mathbf{K}^m. \tag{7}$$

This expansion has a simple interpretation: $\mathbf{K}^m_{ij}$ represents paths from a neuron i to neuron j that are exactly m synapses long (with synaptic weights $\mathbf{W}$ weighted by the postsynaptic response gain $\mathbf{A}$) [37••,38•]. Using this expansion in Equation 6, without external input, also provides an intuitive description of the spike train cross-spectra in terms of paths through the network,

$$\mathbf{C}_{ij} \approx \sum_{m=0}^{X}\sum_{n=0}^{Y}\sum_{k} \underbrace{(\mathbf{K}^m)_{ik}(\mathbf{K}^*)^n_{kj}}_{\text{path terms}} \mathbf{C}^0_{kk}. \tag{8}$$

This expression explicitly captures contribution to the cross-spectrum, $\mathbf{C}_{ij}$, of all paths of up to X synapses ending at neuron i, and all paths of up to Y synapses ending at neuron j. The index k runs over all neurons. A first step toward the path expansion was taken by Ostojic, Brunel & Hakim, who explored the first-order truncation of Equation 6 for two cells, thus capturing contributions from direct connections and common inputs [39]. In multi-cell circuits, different orders of Equation 8 reveal the contributions of different length paths through the network (Box 1, panel B).

The relationship of spike train cross-spectra to pathways through the network provides a powerful tool for understanding how network connectivity shapes population-wide network activity. The population power spectrum is given by the average over the cross-spectral matrix: $C = \langle \mathrm{C}_{ij} \rangle_{i,j}$ (the subscripts on the angular brackets denote averaging over pairs of neurons within a given network; Box 1). Therefore $C(\omega)$ is the average of the left-hand side of Equation 8. The right-hand side of Equation 8 can in turn be linked to the *motif moments* that describe the mean strength of different weighted microcircuits in the network.

Assuming cellular response properties are homogeneous, the interaction matrix can be written as $\mathbf{K} = A\mathbf{W}$, where the scalar kernel A is the same response kernel for all cells. If the baseline auto-correlations, hence $\mathbf{C}^0_{kk}$, are also equal across the network, the 'path terms' appearing in Equation 8 are directly proportional to the *motif moments* of the connectivity matrix $\mathbf{W}$, defined as:

$$\mu_{m,n} = \langle \mathbf{W}^m \left(\mathbf{W}^T\right)^n \rangle_{i,j} / N^{m+n+1}. \tag{9}$$

This measures the average strength of a (m, n)–motif composed of two paths of synapses emanating from a neuron k with one path of m synapses ending at neuron i, the other path of n synapses ending at neuron j. Examples of a (1, 1)-motif, and (1, 2)-motif are shown in Figure 1a. For networks where $\mathrm{W}_{ij} = 0$ or 1, $\mu_{m,n}$ is also the frequency of observing a motif in the network. Equation 8 thus provides a way to approximate how average correlations depend on the frequency of motifs in the network.

An accurate approximation of the population power spectrum typically requires knowledge of many-synapse motifs (Figure 1c), which are difficult to measure experimentally. Importantly, however, the contribution of higher-order motifs can often be decomposed into contributions of smaller, component motifs by introducing *motif cumulants* (Figure 1b) [52••,53•]. This approach allows us to remove redundancies in motif statistics, and isolate the impact solely due to higher order motif structure. A motif cumulant expansion allows Equation 8 to be re-arranged in order to only truncate higher-order motif

Figure 1

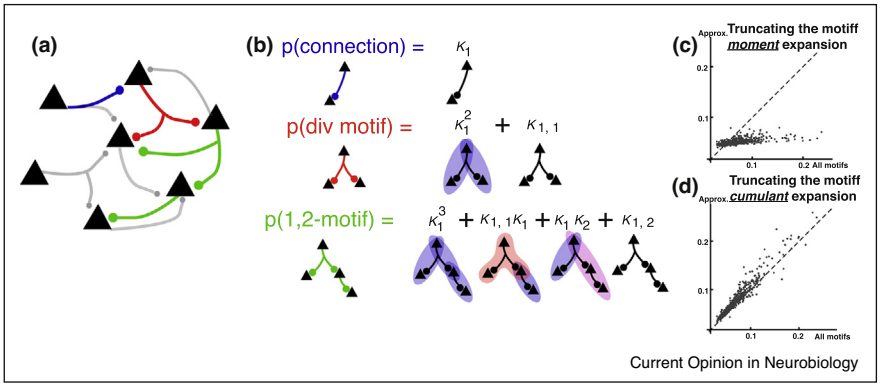

(a) Various motifs are identified throughout the neural network. Their frequency can be measured by counting their occurrence. **(b)** The probability of a motif (motif moments $\mu_{m,n}$, see text) can be decomposed into cumulants of smaller motifs. **(c)** Comparing the average correlation between excitatory neurons calculated using motif statistics of all orders ($X, Y \to \infty$ in Equation 8) and approximations using up to second order ($X + Y \leq 2$) for 512 networks (different dots) with various motif structures. Each network is composed of 80 excitatory and 20 inhibitory neurons. The deviation from the dashed line $y = x$ shows that motif moments beyond second order are needed to accurately describe correlations. **(d)** Same as (c) for a motif cumulant expansion (Eqn 44 in [52••], a generalization of the motif cumulant theory for networks with multiple neuron populations) truncated after second order motif terms; both panels adapted from [52••].

cumulants, rather than moments, providing a much-improved estimation of the spike train covariances (Figure 1c versus d, [52••]) that is still based only on very small motifs. This provides an efficient link between *local* connectivity structures and population-wide activity.

This theory provides a link between the connectomics of anatomically reconstructed neural circuits and their internally-generated correlations. Whether its predictions are consistent with new joint measurements of circuit activity and structure will be a powerful test. Significant motif cumulant structure exists in local networks of both cortex [54,55] and area CA3 of the hippocampus, where it has been suggested to play a crucial role in pattern completion [56]. This decomposition could also be used to estimate constraints on the possible functional network structures from recorded spike train correlations. Finally as we will see in Sec. 6, correlations in turn can shape a network's motif structure through synaptic plasticity. Measurements of connectivity patterns amongst small numbers of neurons could thus constrain predictions for the evolution of network structure and activity.

Higher-order correlations and network structure

While we have discussed how network structure gives rise to correlations in pairs of spike trains, joint activity in larger groups of neurons, described by higher-order correlations, can significantly affect population activity [57–59]. Analogous results to Equation 6 exist for higher-order correlations in stochastically spiking models [26••,47,60,61]. Network structure has been linked to the strength of third-order correlations in networks with narrow degree distributions [62••], and the allied motif cumulant theory developed [63], advancing the aim of understanding how local connectivity structure impacts higher-order correlations across networks. Finally, a range of work has characterized the statistics of avalanches of neuronal activity: population bursts with power law size distributions [64], which potentially suggest a network operating near an instability [65].

Motifs and stability

The results discussed so far rely on an expansion of activity around a baseline state where neurons fire asynchronously. How such states arise is a question addressed in part by the mean-field theory of spiking networks [29,31••,66,67,68••,69•]. The existence of a stable stationary state depends on the structure of connectivity between neurons. In particular, when connectivity is strong and neurons have heterogeneous in-degrees, the existence of a stable mean-field solution can be lost [70,71]. One way to rescue a stable activity regime is to introduce correlations between neurons' in and out-degrees [70]; these correspond to chain motifs (κ_2 in Figure 1b). Therefore the motifs that control correlated variability also affect the stability of asynchronous balanced states.

Motif structure also affects oscillatory population activity. Roxin showed that in a rate model generating oscillations of the population activity, the variance of in-degrees (related to the strength of convergent motifs) controls the onset of oscillations [72]. Zhao *et al.* took a complementary approach of examining the stability of completely asynchronous and completely synchronous states, showing that two-synapse chains and convergent pairs of inputs regulate the stability of synchronous activity [73••].

Spatial scale of connectivity and inputs determines correlations in large networks

Cortical neurons receive strong external and recurrent excitatory projections that could, if left unchecked, drive neuronal activity to saturated levels. Fortunately, strong recurrent inhibition *balances* excitation, acting to stabilize cortical activity and allow moderate firing. These large and balanced inhibitory and excitatory inputs are a major source of synaptic fluctuations, ultimately generating output spiking activity with Poisson-like variability [74,75].

A central feature of balanced networks is that they produce *asynchronous*, uncorrelated spiking activity (in the limit of large networks). Original treatments of balanced networks by van Vreeswijk and Sompolinsky [29,30] and Amit and Brunel [76] explained asynchronous activity by assuming sparse wiring within the network, so that shared inputs between neurons were negligible. Renart, de la Rocha, Harris and colleagues showed that homogeneous balanced networks admit an asynchronous solution despite dense wiring [31••] (for large networks). This result suggests a much deeper relationship between balance and asynchronous activity than previously realized. Building on this work, Rosenbaum, Doiron and colleagues extended the theory of balanced networks to include spatially dependent connectivity [16••,77]. We review below how the spatial spread of connectivity provides new routes to correlated activity in balanced networks.

Consider a two-layer network, with the second layer receiving both feedforward (F) and recurrent (R) inputs (Figure 2a). Assume that the second layer is composed of both excitatory and inhibitory neurons, so that R contains excitatory and inhibitory synaptic inputs. The feedforward pathway can then include both excitation and inhibition, or only one of the two. For simplicity, we assume that the widths of recurrent excitation and inhibition are equal and take the feedforward and recurrent projections to have Gaussian profiles with widths σ_F and σ_R, respectively. Each neuron thus receives the combined input $I = F + R$. Considering a representative pair of layer two neurons separated by a distance d, this yields a decomposition of their inputs' covariance C_{II} as:

$$C_{II}(d) = C_{FF}(d) + C_{RR}(d) + 2C_{RF}(d). \tag{10}$$

Here C_{FF} and C_{RR} are the covariances of the feedforward and recurrent portions of the two neurons' inputs, respectively, while C_{RF} is the indirect contribution to covariance from the recurrent pathway tracking the feedforward pathway.

If the network coupling is dense and the first-layer neurons are uncorrelated with one another then C_{FF}, C_{RR} and C_{RF} are all $O(1)$. This means that feedforward and recurrent projections are potential sources of correlations within the network. The asynchronous state requires that $C_{II} \sim O(1/N)$. This can only be true if the feedforward and recurrent correlations are *balanced* so that the recurrent pathway tracks and cancels the correlations due to the feedfoward pathway. If we take $N \to \infty$ then in the asynchronous state, $C(d) \to 0$ implies:

$$C_{RF}(d) = -\frac{1}{2}(C_{FF}(d) + C_{RR}(d)). \tag{11}$$

This must be true for *every distance d*, and from Equation 10 we derive [16••] that the various spatial scales must satisfy:

$$\sigma_F^2 = \sigma_R^2 + \sigma_{\text{rate}}^2. \tag{12}$$

Here σ_{rate}^2 is the spatial scale of correlated firing within the network. The intuition here is that for cancellation at every d the spatial scale of feedforward and recurrent correlations must match one another. While the spatial scale of $C_{FF}(d)$ is determined only by σ_F, the scale of recurrent correlations is calculated from the correlated spiking activity convolved with the recurrent coupling (hence the sum $\sigma_R^2 + \sigma_{\text{rate}}^2$). While σ_F and σ_R are architectural parameters of the circuit (and hence fixed), σ_{rate} is a model output that must be determined. For any solution to make sense we require that $\sigma_{\text{rate}} > 0$. This gives a compact asynchrony condition: $\sigma_F > \sigma_R$. In other words for feedforward and recurrent correlations to cancel, the spatial spread of feedforward projections must be larger than the spatial spread of recurrent projections.

To illustrate how the spatial scales of connectivity control the asynchronous solution, we analyze the activity of a balanced spiking network when $\sigma_F > \sigma_R$ is satisfied (Figure 2b1, left). As expected, the spiking activity is roughly asynchronous with spike count correlations near zero (Figure 2b1, middle). While they are not identically zero, the correlations approach zero as network size increases, if $\sigma_F > \sigma_R$ [16••]. When we examine the contributions of the feedforward and recurrent pathways, we see that the relation in Equation 11 is satisfied (Figure 2b1, right). We contrast this to the case when $\sigma_F < \sigma_R$, violating the asynchrony condition (Figure 2b2, left). Here, a clear signature of correlations is found: neuron that are nearby one another are positively correlated while more distant neuron pairs are negatively correlated. Crucially, these correlations do not vanish in the limit of large networks [16••].

Layer 2/3 of macaque visual area V1 is expected to have $\sigma_F < \sigma_R$, with long range projections within 2/3 being broader than L4 projections to L2/3 [78,79]. Smith and Kohn collected population activity over large distances in

Figure 2

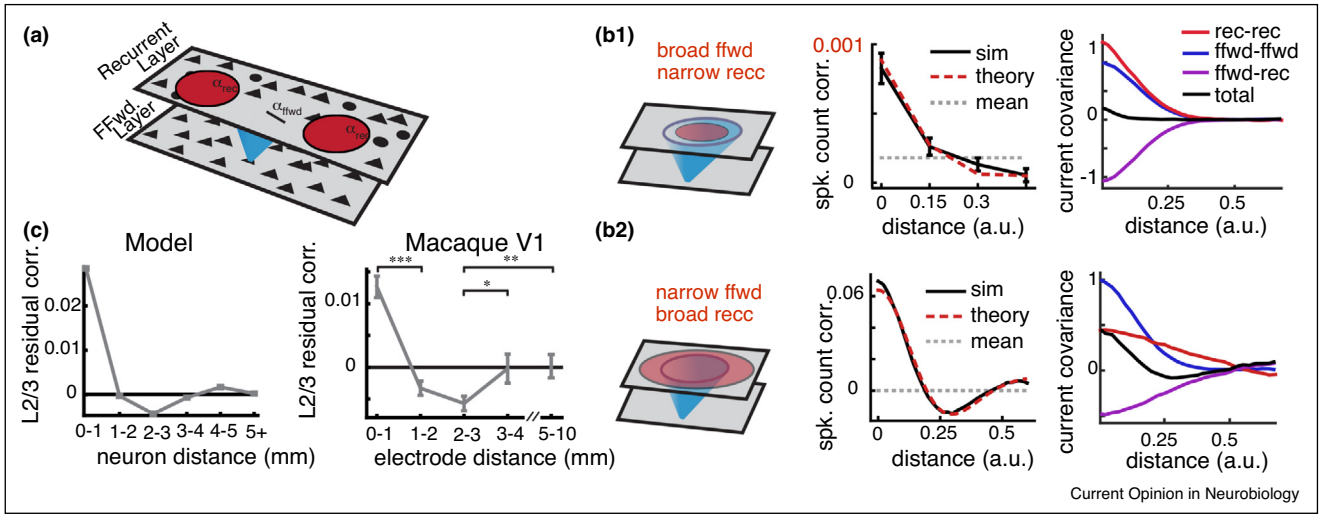

Correlated activity in balanced networks with spatially dependent connections. **(a)** Schematic of the two layer network. The blue/red zones denotes the spatial scale of feedforward/recurrent connectivity. **(b1)** Broad feedforward and narrow recurrent connectivity (left) produce an asynchronous state (middle). The asynchrony requires a cancellation of $C_{RR}(d)$ and $C_{FF}(d)$ by $C_{RF}(d)$ at all distances (right). **(b2)** Narrow feedforward and broad recurrent connectivity (left) produce spatially structured correlations (middle) because $C_{RF}(d)$ does not cancel $C_{RR}(d)$ and $C_{FF}(d)$ (right). **(c)** When a one-dimensional latent variable is extracted and removed from the primate V1 array data, the model predictions (left) are validated (right). Panels are from [16••].

layer 2/3 of macaque V1 [80]. When a low-rank source of correlations (putatively corresponding to the external term of Equation 6), the spatial signature predicted above is revealed (Figure 2c).

While these arguments give conditions for when the asynchronous solution will exist, it cannot give an estimate of correlated activity. Rather, when either $N<\infty$ or $\sigma_F < \sigma_R$, we require the linear response formulation of Equation 6 to give a prediction of how network correlations scale with distance (red dashed in Figure 2b1 and b2, middle). It is interesting to note that a majority of the fluctuations are internally generated within the balanced circuit and subsequently have a rich spectrum of timescales. For spikes counted over long windows, the linear response formalism of Equation 6 once again predicts the underlying correlations ('theory curves').

Joint activity drives plasticity of recurrent connectivity

The structure of neuronal networks is plastic, with synapses potentiating or depressing in a way that depends on pre- and postsynaptic spiking activity [81]. When synaptic plasticity is slow compared to the timescales of spiking dynamics, changes in synaptic weights are linked to the *statistics* of the spike trains [82]:

$$\mathbf{W}_{ij} = f\big(\mathbf{m}_i(t_i), \mathbf{m}_j(t_j)\big) + g\big(\mathbf{m}_{ij}(t_i,t_j)\big) + h\big(\mathbf{m}_{ijk}(t_i,t_j,t_k)\big) + \dots \quad (13)$$

where $\dot{\mathbf{W}}$ denotes the dynamics of the connectivity matrix $\mathbf{W}$ on the slow timescale of plasticity. f determines the weight changes due to individual presynaptic and postsynaptic spikes, g determines weight changes due to pairs of spikes, h weight changes due to spike triplets, and so on. For plasticity rules based on pairs of presynaptic and postsynaptic spikes, this results in a joint evolution of the weight matrix $\mathbf{W}$, the firing rates, $\vec{\mathbf{r}}$, and the cross-covariances, $\mathbf{C}$ (Figure 3a–c).

As we saw above, spike train cumulants depend on the network structure. In the presence of plasticity mechanisms, the structure of neuronal networks thus controls its own evolution — both directly by generating correlations [8••,9] and indirectly, by filtering the correlations inherited from external sources [83••,84]. Recent work has leveraged this connection to determine how particular structural motifs shape spike train correlations to drive plasticity [9]. A further step is to close the loop on motifs, leveraging approximations of the true spike-train correlations in order to predict the plasticity dynamics of motif statistics. The definitions of motif moments and cumulants involve an average over the population (Equation 9). This links their plasticity to the average spike train moments across the population, allowing the derivation of dynamical rules governing the plasticity, not of individual synapses, but of the average strength of connectivity motifs [8••,84]:

$$\dot{\vec{\kappa}} = F(\mathbf{m}(\vec{\kappa}, \mathbf{C}^{\text{ext}})), \quad (14)$$

Figure 3

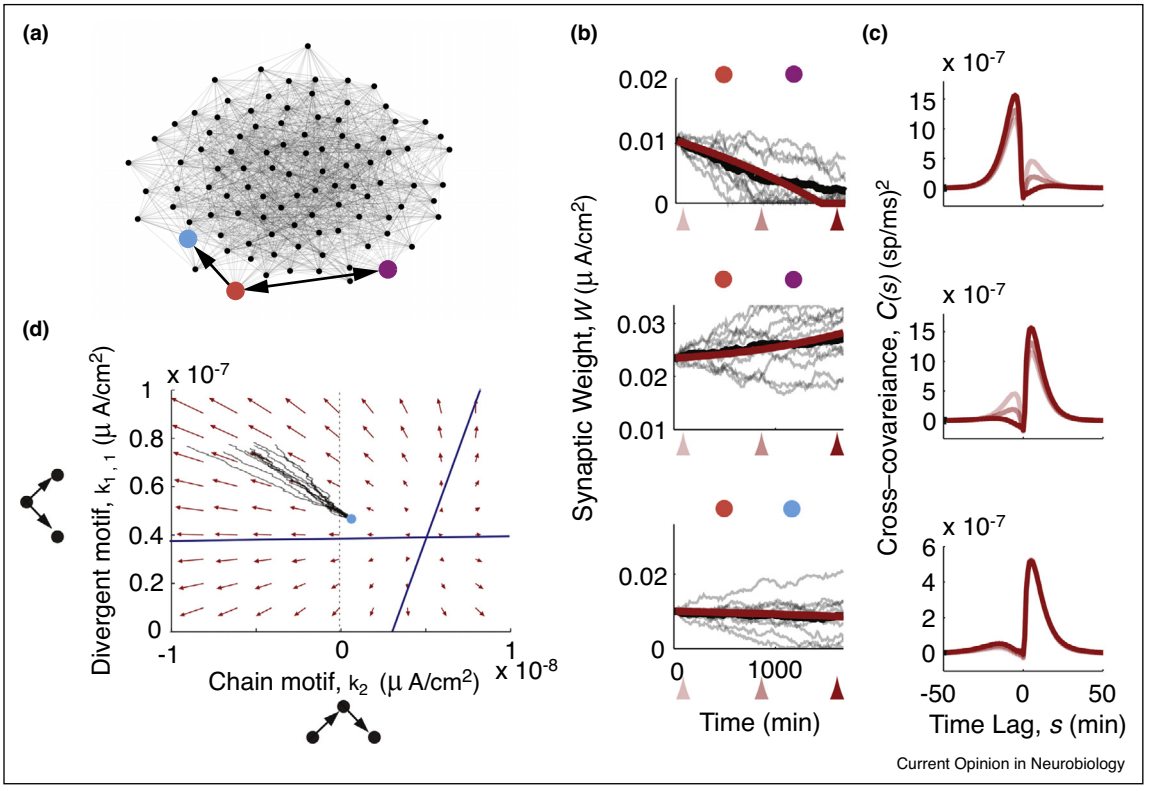

Spike timing-dependent plasticity gives rise to joint evolution of synaptic weights, spike train covariances, and motif statistics. Panels from [8••]. **(a)** Diagram of network structure. **(b)** Evolution of the three synapses highlighted in panel A. Red: theoretical prediction. Gray: evolution of synaptic weights on individual trials. Black: trial-averaged synaptic weight. **(c)** Evolution of the spike train covariances between the presynaptic and postsynaptic cells of each synapse, predicted using the first-order truncation of Equation 8. Shading corresponds to the time points marked with arrows below the time axis of panel B. As synaptic weights potentiate or depress, the causal 'bumps' they contribute to the spike train covariance grows or shrinks. **(d)** Projection of the joint dynamics of two-synapse motif cumulants into the (divergent, chain) plane under a pair-based, additive Hebbian plasticity rule.

where $\vec{\kappa}$ represents a chosen set of motif cumulants and the form of the function F depends on the plasticity model used.

One such analysis reveals that under an additive, pair-based plasticity rule where pre-post pairs cause potentiation and post-pre pairs cause depression, an unstructured weight matrix (with zero motif cumulants) is unstable: the average strength of motifs will spontaneously potentiate or depress, creating structure in the synaptic weights (Figure 3d), [8••]. So far, such studies have focused on plasticity driven by spike pairs, relying on the linear response theories of [37••,38•,43]. More biologically realistic plasticity models rely on multi-spike interactions and variables measuring postsynaptic voltage or calcium concentrations [7]. Theories describing higher-order spike-train and spike-voltage or spike-calcium correlations will provide a new window through which to examine networks endowed with these richer plasticity rules.

Conclusion

The next few years could be pivotal for the study of how network structure drives neural dynamics. Spectacular experimental methods are producing vast datasets that unite connectivity and activity data in new ways [14,21,19,23]. Does our field have a theory equal to the data? We've reviewed how mathematical tools can separate the two main mechanisms giving rise to collective spiking activity — recurrent connectivity and common inputs — and noted how this connects with decomposition methods in data analysis [15,16••,17,35]. Moreover, we are beginning to understand how local and spatial structures scale up to global activity patterns, and how they drive network plasticity. Exciting applications of these theories await, linking anatomical and functional structure in recorded and reconstructed neural circuits and elucidating the impact of newly discovered cell types' intrinsic dynamics and connectivity profiles on population activity and computations. The theories we presented

rely, however, on the existence of stable activity states and on simple point-neuron models. Daunting challenges thus remain, from linking network structure with nonlinear and non-stationary single-neuron and network dynamics to bridging the spatial scales of single-neuron anatomy with point-neuron models. As the bar ratchets up ever faster, the field will be watching to see what theories manage to clear it.

Conflict of interest statement

Nothing declared.

Acknowledgements

We acknowledge the support of the NSF through grants DMS-1514743 and DMS-1056125 (ESB), DMS-1313225 and DMS-1517082 (B.D.), DMS-1517629 (KJ), DMS-1517828 (R.R.) and NSF/NIGMS-R01GM104974 (KJ), as well as the Simons Fellowships in Mathematics (ESB and KJ). GO, MB, and ESB wish to thank the Allen Institute founders, Paul G. Allen and Jody Allen, for their vision, encouragement and support.

References and recommended reading

Papers of particular interest, published within the period of review, have been highlighted as:

- • of special interest
- •• of outstanding interest

1. Dettner A, Münzberg S, Tchumatchenko T: **Temporal pairwise spike correlations fully capture single-neuron information**. *Nat Commun* 2016, **7**:13805 http://dx.doi.org/10.1038/ncomms13805.

2. Hu Y, Zylberberg J, Shea-Brown E: **The sign rule and beyond: boundary effects, flexibility, and noise correlations in neural population codes**. *PLoS Comput Biol* 2014, **10**:e1003469 http://dx.doi.org/10.1371/journal.pcbi.1003469.

3. Moreno-Bote R, Beck J, Kanitscheider I, Pitkow X, Latham P, Pouget A: **Information-limiting correlations**. *Nat Neurosci* 2014, **17**:1410-1417 http://dx.doi.org/10.1038/nn.3807.

4. Zylberberg J, Cafaro J, Turner MH, Shea-Brown E, Rieke F: **Direction-selective circuits shape noise to ensure a precise population code**. *Neuron* 2016, **89**:369-383 http://dx.doi.org/10.1016/j.neuron.2015.11.019.

5. Franke F, Fiscella M, Sevelev M, Roska B, Hierlemann A, Azeredo da Silveira R: **Structures of neural correlation and how they favor coding**. *Neuron* 2016, **89**:409-422 http://dx.doi.org/10.1016/j.neuron.2015.12.037.

6. Kumar A, Rotter S, Aertsen A: **Spiking activity propagation in neuronal networks: reconciling different perspectives on neural coding**. *Nat Rev Neurosci* 2010, **11**:615-627.

7. Markram H, Gerstner W, Sjöström PJ: **A history of spike-timing-dependent plasticity**. *Front Synaptic Neurosci* 2011, **3**:4 http://dx.doi.org/10.3389/fnsyn.2011.00004.

8. •• Ocker GK, Litwin-Kumar A, Doiron B: **Self-organization of microcircuits in networks of spiking neurons with plastic synapses**. *PLoS Comput Biol* 2015, **11**:e1004458 http://dx.doi.org/10.1371/journal.pcbi.1004458.
Uses the linear response theory for integrate-and-fire neurons to construct self-consistent predictions for internally-generated correlations and synaptic plasticity, and then derive a reduced dynamics for the spike timing-dependent plasticity of 2-synapse motif cumulants. This shows that an initially unstructured (Erdős-Rènyi) network connectivity is unstable under additive, Hebbian STDP unless all synapses potentiate or depress together.

9. Tannenbaum NR, Burak Y: **Shaping neural circuits by high order synaptic interactions**. *PLoS Comput Biol* 2016, **12**:e1005056 http://dx.doi.org/10.1371/journal.pcbi.1005056.

10. Graupner M, Wallisch P, Ostojic S: **Natural firing patterns imply low sensitivity of synaptic plasticity to spike timing compared with firing rate**. *J Neurosci* 2016, **36**:11238-11258 http://dx.doi.org/10.1523/JNEUROSCI. 0104-16.2016.

11. Cohen MR, Kohn A: **Measuring and interpreting neuronal correlations**. *Nat Neurosci* 2011, **14**:811-819 http://dx.doi.org/10.1038/nn.2842.

12. McGinley MJ, Vinck M, Reimer J, Batista-Brito R, Zagha E, Cadwell CR *et al.*: **Waking state: rapid variations modulate neural and behavioral responses**. *Neuron* 2015, **87**:1143-1161 http://dx.doi.org/10.1016/j.neuron.2015.09.012.

13. Doiron B, Litwin-Kumar A, Rosenbaum R, Ocker GK, Josić K: **The mechanics of state-dependent neural correlations**. *Nat Neurosci* 2016, **19**:383-393 http://dx.doi.org/10.1038/nn.4242.

14. Cossell L, Iacaruso MF, Muir DR, Houlton R, Sader EN, Ko H *et al.*: **Functional organization of excitatory synaptic strength in primary visual cortex**. *Nature* 2015, **518**:399-403 http://dx.doi.org/10.1038/nature14182.

15. Ecker A, Berens P, Cotton RJ, Subramaniyan M, Denfield G, Cadwell C *et al.*: **State dependence of noise correlations in macaque primary visual cortex**. *Neuron* 2014, **82**:235-248 http://dx.doi.org/10.1016/j.neuron.2014.02.006.

16. •• Rosenbaum R, Smith MA, Kohn A, Rubin JE, Doiron B: **The spatial structure of correlated neuronal variability**. *Nat Neurosci* 2017, **20**:107-114 http://dx.doi.org/10.1038/nn.4433.
Building on their 2014 work in PRX, the authors extends the theory of correlations in balanced networks to systems with spatially dependent connectivity, showing that mismatches in the spatial scales of feedforward and recurrent inputs can give rise to stable average firing rates but significant spike correlations.

17. Goris RLT, Movshon JA, Simoncelli EP: **Partitioning neuronal variability**. *Nat Neurosci* 2014, **17**:858-865 http://dx.doi.org/10.1038/nn.3711.

18. Ecker AS, Denfield GH, Bethge M, Tolias AS: **On the structure of neuronal population activity under fluctuations in attentional state**. *J Neurosci* 2016, **36**:1775-1789 http://dx.doi.org/10.1523/JNEUROSCI. 2044-15.2016.

19. Lee WCA, Bonin V, Reed M, Graham BJ, Hood G, Glattfelder K *et al.*: **Anatomy and function of an excitatory network in the visual cortex**. *Nature* 2016, **532**:370-374 http://dx.doi.org/10.1038/nature17192.

20. Kasthuri N, Hayworth KJ, Berger DR, Schalek RL, Conchello JA, Knowles-Barley S *et al.*: **Saturated reconstruction of a volume of neocortex**. *Cell* 2015, **162**:648-661 http://dx.doi.org/10.1016/j.cell.2015.06.054.

21. Bock DD, Lee WCA, Kerlin AM, Andermann ML, Hood G, Wetzel AW *et al.*: **Network anatomy and in vivo physiology of visual cortical neurons**. *Nature* 2011, **471**:177-182 http://dx.doi.org/10.1038/nature09802.

22. Kleinfeld D, Bharioke A, Blinder P, Bock DD, Briggman KL, Chklovskii DB *et al.*: **Large-scale automated histology in the pursuit of connectomes**. *J Neurosci* 2011, **31**:16125-16138 http://dx.doi.org/10.1523/JNEUROSCI. 4077-11.2011.

23. Briggman KL, Helmstaedter M, Denk W: **Wiring specificity in the direction-selectivity circuit of the retina**. *Nature* 2011, **471**:183-188 http://dx.doi.org/10.1038/nature09818.

24. Helmstaedter M, Briggman KL, Turaga SC, Jain V, Seung HS, Denk W: **Connectomic reconstruction of the inner plexiform layer in the mouse retina**. *Nature* 2013, **500**:168-174 http://dx.doi.org/10.1038/nature12346.

25. Mishchenko Y, Hu T, Spacek J, Mendenhall J, Harris KM, Chklovskii DB: **Ultrastructural analysis of hippocampal neuropil from the connectomics perspective**. *Neuron* 2010, **67**:1009-1020 http://dx.doi.org/10.1016/j.neuron.2010.08.014.

26. •• Ocker GK, Josić K, Shea-Brown E, Buice MA: **Linking structure and activity in nonlinear spiking networks**. *PLoS Comput Biol* 2017, **13**:e1005583 http://dx.doi.org/10.1371/journal.pcbi.1005583.
Extends existing theories for spike correlations to allow for nonlinear interactions among inputs and firing rates, deriving series of 'diagrams' that show how connectivity influences activity statistics for quadratic and higher orders firing rate responses.

27. Novak J, LaCroix M: *Three lectures on free probability*. 2012. arXiv:12052097 [math-ph].

28. Faisal AA, Selen LPJ, Wolpert DM: **Noise in the nervous system**. *Nat Rev Neurosci* 2008, **9**:292-303 http://dx.doi.org/10.1038/nrn2258.

29. van Vreeswijk C, Sompolinsky H: **Chaos in neuronal networks with balanced excitatory and inhibitory activity**. *Science* 1996, **274**:1724-1726.

30. van Vreeswijk C, Sompolinsky H: **Chaotic balanced state in a model of cortical circuits**. *Neural Comput* 1998, **10**:1321-1371.

31. •• Renart A, Rocha Jdl, Bartho P, Hollender L, Parga N, Reyes A *et al.*: **The asynchronous state in cortical circuits**. *Science* 2010, **327**:587-590 http://dx.doi.org/10.1126/science.1179850.
Shows that for balanced networks with dense and strong connectivity, an asynchronous state emerges in the large-N limit in which excitatory–inhibitory interactions dynamically cancel excitatory–excitatory and inhibitory–inhibitory correlations. This leads to spike correlations that vanish on average. Also in the large N limit, this arises from population responses that instantaneously and linearly track external inputs.

32. de la Rocha J, Doiron B, Shea-Brown E, Josić K, Reyes A: **Correlation between neural spike trains increases with firing rate**. *Nature* 2007, **448**:802-806 http://dx.doi.org/10.1038/nature06028.

33. Bair W, Zohary E, Newsome WT: **Correlated firing in macaque visual area MT: time scales and relationship to behavior**. *J Neurosci* 2001, **21**:1676-1697.

34. Gabbiani F, Cox SJ: *Mathematics for neuroscientists*. Academic Press; 2010.

35. Yatsenko D, Josić K, Ecker AS, Froudarakis E, Cotton RJ, Tolias AS: **Improved estimation and interpretation of correlations in neural circuits**. *PLoS Comput Biol* 2015, **11**: e1004083 http://dx.doi.org/10.1371/journal.pcbi.1004083.

36. Shea-Brown E, Josić K, de la Rocha J, Doiron B: **Correlation and synchrony transfer in integrate-and-fire neurons: basic properties and consequences for coding**. *Phys Rev Lett* 2008, **100**.

37. •• Pernice V, Staude B, Cardanobile S, Rotter S: **How structure determines correlations in neuronal networks**. *PLoS Comput Biol* 2011, **7**:e1002059 http://dx.doi.org/10.1371/journal.pcbi.1002059.
Calculates the full matrix of pairwise correlation functions either in networks of interacting Poisson (Hawkes process) neurons. Shows how network-wide correlation is related to connectivity paths and motifs.

38. • Trousdale J, Hu Y, Shea-Brown E, Josić K: **Impact of network structure and cellular response on spike time correlations**. *PLoS Comput Biol* 2012, **8**:e1002408 http://dx.doi.org/10.1371/journal.pcbi.1002408.
Calculates the linear response predictions for the full matrix of pairwise correlation functions, and their relationship to connectivity paths, in networks of integrate-and-fire neurons.

39. Ostojic S, Brunel N, Hakim V: **How connectivity, background activity, and synaptic properties shape the cross-correlation between spike trains**. *J Neurosci* 2009, **29**:10234-10253.

40. Sejnowski TJ: **On the stochastic dynamics of neuronal interaction**. *Biol Cybernet* 1976, **22**:203-211 http://dx.doi.org/10.1007/BF00365086.

41. Doiron B, Lindner B, Longtin A, Maler L, Bastian J: **Oscillatory activity in electrosensory neurons increases with the spatial correlation of the stochastic input stimulus**. *Phys Rev Lett* 2004, **93**.

42. Lindner B, Doiron B, Longtin A: **Theory of oscillatory firing induced by spatially correlated noise and delayed inhibitory feedback**. *Phys Rev E* 2005:2005.

43. Hawkes AG: **Spectra of some self-exciting and mutually exciting point processes**. *Biometrika* 1971, **58**:83-90 http://dx.doi.org/10.1093/biomet/58.1.83.

44. Pernice V, Staude B, Cardanobile S, Rotter S: **Recurrent interactions in spiking networks with arbitrary topology**. *Phys Rev E* 2012, **85**:031916 http://dx.doi.org/10.1103/PhysRevE.85.031916.

45. Grytskyy D, Tetzlaff T, Diesmann M, Helias M: **A unified view on weakly correlated recurrent networks**. *Front Comput Neurosci* 2013, **7** http://dx.doi.org/10.3389/fncom.2013.00131.

46. Ostojic S, Brunel N: **From spiking neuron models to linear–nonlinear models**. *PLoS Comput Biol* 2011, **7**:e1001056 http://dx.doi.org/10.1371/journal.pcbi.1001056.

47. Buice MA, Chow CC, Cowan JD: **Systematic fluctuation expansion for neural network activity equations**. *Neural Comput* 2010, **22**:377-426.

48. Hildebrand EJ, Buice MA, Chow CC: **Kinetic theory of coupled oscillators**. *Phys Rev Lett* 2007, **98**:054101 http://dx.doi.org/10.1103/PhysRevLett.98.054101.

49. Buice MA, Chow CC: **Correlations, fluctuations, and stability of a finite-size network of coupled oscillators**. *Phys Rev E* 2007, **76**:031118 http://dx.doi.org/10.1103/PhysRevE.76.031118.

50. Buice MA, Chow CC: **Dynamic finite size effects in spiking neural networks**. *PLoS Comput Biol* 2013, **9**:e1002872 http://dx.doi.org/10.1371/journal.pcbi.1002872.

51. • Rangan AV: **Diagrammatic expansion of pulse-coupled network dynamics**. *Phys Rev Lett* 2009, **102**:158101 http://dx.doi.org/10.1103/PhysRevLett.102.158101.
Develops a diagrammatic expansion for the statistics of stationary integrate-and-fire networks with delta synapses in terms of subnetworks (i.e. motifs) via a functional representation of the full network dynamics (see also the accompanying PRE article).

52. •• Hu Y, Trousdale J, Josić K, Shea-Brown E: **Motif statistics and spike correlations in neuronal networks**. *J Stat Mech: Theory Exp* 2013, **2013**:P03012 http://dx.doi.org/10.1088/1742-5468/2013/03/P03012.
Decomposes the effects of higher order motifs on spike correlations into smaller ones, and show how this *motif cumulant* approach enables one to predict global, population-wide correlations from the statistics of local, two-synapse motifs.

53. • Hu Y, Trousdale J, Josić K, Shea-Brown E: **Local paths to global coherence: cutting networks down to size**. *Phys Rev E* 2014, **89**:032802 http://dx.doi.org/10.1103/PhysRevE.89.032802.
Formulates network motif decompositions via a combinatorial relationship between moments and cumulants, extends the theory to multi-branch motifs related to higher order correlations, and to the impact of heterogeneous connectivity.

54. Song S, Sjöström PJ, Reigl M, Nelson S, Chklovskii DB: **Highly nonrandom features of synaptic connectivity in local cortical circuits**. *PLoS Biol* 2005, **3**:e68 http://dx.doi.org/10.1371/journal.pbio.0030068.

55. Perin R, Berger TK, Markram H: **A synaptic organizing principle for cortical neuronal groups**. *Proc Natl Acad Sci U S A* 2011, **108**:5419-5424 http://dx.doi.org/10.1073/pnas.1016051108.

56. Guzman SJ, Schlögl A, Frotscher M, Jonas P: **Synaptic mechanisms of pattern completion in the hippocampal CA3 network**. *Science* 2016, **353**:1117-1123 http://dx.doi.org/10.1126/science.aaf1836.

57. Ohiorhenuan IE, Mechler F, Purpura KP, Schmid AM, Hu Q, Victor JD: **Sparse coding and high-order correlations in fine-scale cortical networks**. *Nature* 2010, **466**:617-621 http://dx.doi.org/10.1038/nature09178.

58. Shimazaki H, Amari Si, Brown EN, Grün S: **State-space analysis of time-varying higher-order spike correlation for multiple neural spike train data**. *PLoS Comput Biol* 2012, **8**:e1002385 http://dx.doi.org/10.1371/journal.pcbi.1002385.

59. Tkačik G, Marre O, Amodei D, Schneidman E, Bialek W, Ii MJB: **Searching for collective behavior in a large network of sensory neurons**. *PLoS Comput Biol* 2014, **10**:e1003408 http://dx.doi.org/10.1371/journal.pcbi.1003408.

60. Buice MA, Chow CC: **Beyond mean field theory: statistical field theory for neural networks**. *J Stat Mech* 2013, **2013**:P03003 http://dx.doi.org/10.1088/1742-5468/2013/03/P03003.

61. Jovanović S, Hertz J, Rotter S: **Cumulants of Hawkes point processes**. *Phys Rev E* 2015, **91**:042802 http://dx.doi.org/10.1103/PhysRevE.91.042802.

62. •• Jovanović S, Rotter S: **Interplay between graph topology and correlations of third order in spiking neuronal networks**. *PLOS Comput Biol* 2016, **12**:e1004963 http://dx.doi.org/10.1371/journal.pcbi.1004963.
Building on their PRE 2015 paper, calculates the linear response predictions for the *n*th order cumulant densities of multivariate Hawkes processes (i.e. linear-Poisson neural networks), and shows how these are related to connectivity in regular networks (those with narrow degree distributions).

63. Hu Y, Josić K, Shea-Brown E, Buice MA: **From structure to dynamics: origin of higher-order spike correlations in network motifs**. *Cosyne Abstracts*; *Salt Lake City, UT: 2015*.

64. Plenz D, Thiagarajan TC: **The organizing principles of neuronal avalanches: cell assemblies in the cortex?** *Trends Neurosci* 2007, **30**:101-110 http://dx.doi.org/10.1016/j.tins.2007.01.005.

65. Buice MA, Cowan JD: **Field-theoretic approach to fluctuation effects in neural networks**. *Phys Rev E* 2007, **75**:051919 http://dx.doi.org/10.1103/PhysRevE.75.051919.

66. Ginzburg I, Sompolinsky H: **Theory of correlations in stochastic neural networks**. *Phys Rev E* 1994, **50**:3171-3191 http://dx.doi.org/10.1103/PhysRevE.50.3171.

67. Brunel N: **Dynamics of sparsely connected networks of excitatory and inhibitory spiking neurons**. *J Comput Neurosci* 2000, **8**:183-208 http://dx.doi.org/10.1023/A:1008925309027.

68. •• Tetzlaff T, Helias M, Einevoll GT, Diesmann M: **Decorrelation of neural-network activity by inhibitory feedback**. *PLoS Comput Biol* 2012, **8**:e1002596 http://dx.doi.org/10.1371/journal.pcbi.1002596.
A highly complementary study to the more well-known work of Renart *et al.* Using linear response theory for finite-size integrate-and-fire networks, Tetzlaff, Helias *et al*. expose negative feedback loops in the dynamics of both purely inhibitory and excitatory-inhibitory networks, which give rise to the dynamical cancellation of correlations in finite-size networks.

69. • Helias M, Tetzlaff T, Diesmann M: **The correlation structure of local neuronal networks intrinsically results from recurrent dynamics**. *PLoS Comput Biol* 2014, **10**:e1003428 http://dx.doi.org/10.1371/journal.pcbi.1003428.
Building on the study of Renart, de la Rocha *et al.* and on their previous work, the authors disentangle correlation cancellation by excitatory–inhibitory interactions (reflected in the suppression of fluctuations in the population activity) from the tracking of external inputs.

70. Pyle R, Rosenbaum R: **Highly connected neurons spike less frequently in balanced networks**. *Phys Rev E* 2016, **93** http://dx.doi.org/10.1103/PhysRevE.93.040302.

71. Landau ID, Egger R, Dercksen VJ, Oberlaender M, Sompolinsky H: **The impact of structural heterogeneity on excitation-inhibition balance in cortical networks**. *Neuron* 2016, **0** http://dx.doi.org/10.1016/j.neuron.2016.10.027.

72. Roxin A: **The role of degree distribution in shaping the dynamics in networks of sparsely connected spiking neurons**. *Front Comput Neurosci* 2011, **5**:8 http://dx.doi.org/10.3389/fncom.2011.00008.

73. •• Zhao L, Beverlin BI, Netoff T, Nykamp DQ: **Synchronization from second order network connectivity statistics**. *Front Comput Neurosci* 2011, **5**:28 http://dx.doi.org/10.3389/fncom.2011.00028.
A pioneering study of how network motifs impact network-wide synchrony, including simulations, analytical results, and methods of generating useful networks to test theories linking structure to activity.

74. Doiron B, Litwin-Kumar A: **Balanced neural architecture and the idling brain**. *Front Comput Neurosci* 2014, **8** http://dx.doi.org/10.3389/fncom.2014.00056.

75. Denève S, Machens CK: **Efficient codes and balanced networks**. *Nat Neurosci* 2016, **19**:375-382 http://dx.doi.org/10.1038/nn.4243.

76. Amit DJ, Brunel N: **Model of global spontaneous activity and local structured activity during delay periods in the cerebral cortex**. *Cereb Cortex* 1997, **7**:237-252.

77. Rosenbaum R, Doiron B: **Balanced networks of spiking neurons with spatially dependent recurrent connections**. *Phys Rev X* 2014, **4**:021039 http://dx.doi.org/10.1103/PhysRevX.4.021039.

78. Bosking WH, Zhang Y, Schofield B, Fitzpatrick D: **Orientation selectivity and the arrangement of horizontal connections in tree shrew striate cortex**. *J Neurosci* 1997, **17**:2112-2127.

79. Lund JS, Angelucci A, Bressloff PC: **Anatomical substrates for functional columns in macaque monkey primary visual cortex**. *Cereb Cortex* 2003, **13**:15-24 http://dx.doi.org/10.1093/cercor/13.1.15.

80. Smith MA, Kohn A: **Spatial and temporal scales of neuronal correlation in primary visual cortex**. *J Neurosci* 2008, **28**:12591-12603 http://dx.doi.org/10.1523/JNEUROSCI. 2929-08.2008.

81. Feldman D: **The spike-timing dependence of plasticity**. *Neuron* 2012, **75**:556-571 http://dx.doi.org/10.1016/j.neuron.2012.08.001.

82. Gerstner W, Kistler WM: **Mathematical formulations of Hebbian learning**. *Biol Cybernet* 2002, **87**:404-415 http://dx.doi.org/10.1007/s00422-002-0353-y.

83. •• Gilson M, Burkitt AN, Grayden DB, Thomas DA, Hemmen JL: **Emergence of network structure due to spike-timing-dependent plasticity in recurrent neuronal networks IV: structuring synaptic pathways among recurrent connections**. *Biol Cybernet* 2009, **101**:427-444 http://dx.doi.org/10.1007/s00422-009-0346-1.
Building on the authors' previous work on STDP in networks of Poisson neurons (Gilson *et al.*, Biol. Cyb. 2009-iii), uses a combination of the Hawkes theory and a mean-field calculation of synaptic weights to show that externally-generated correlations can give rise to selective connectivity in recurrent networks of Poisson neurons through spike timing-dependent plasticity.

84. Ocker GK, Doiron B: *Training and spontaneous reinforcement of neuronal assemblies by spike timing*. 2016. arXiv:160800064 [q-bio].

85. Dummer B, Wieland S, Lindner B: **Self-consistent determination of the spike-train power spectrum in a neural network with sparse connectivity**. *Front Comput Neurosci* 2014, **8**:104.

86. Schwalger T, Droste F, Lindner B: **Statistical structure of neural spiking under non-Poissonian or other non-white stimulation**. *J Comput Neurosci* 2015, **39**:29-51.

87. Wieland S, Bernardi D, Schwalger T, Lindner B: **Slow fluctuations in recurrent networks of spiking neurons**. *Phys Rev E* 2015, **92**:040901.

88. Ostojic S: **Two types of asynchronous activity in networks of excitatory and inhibitory spiking neurons**. *Nat Neurosci* 2014, **17**:594-600.

89. Leen DA, Shea-Brown E: **A simple mechanism for beyond-pairwise correlations in integrate-and-fire**. *Neurons J Math Neurosci* 2015, **5**:17.

90. Kruscha A, Lindner B: **Spike-count distribution in a neuronal population under weak common stimulation**. *Phys Rev E* 2015, **92**:052817.

91. Harish O, Hansel D: **Asynchronous rate chaos in spiking neuronal circuits**. *PLOS Comput Biol* 2015, **11**:e1004266.

92. Mastrogiuseppe F, Ostojic S: **Intrinsically-generated fluctuating activity in excitatory-inhibitory networks**. *PLOS Comput Biol* 2017, **13**:e1005498.